Fuel 324 (2022) 124779

Contents lists available at ScienceDirect

Fuel

journal homepage: www.elsevier.com/locate/fuel

Full Length Article

Design and optimization of multigeneration biogas power plant using waste heat recovery System: A case study with Energy, Exergy, and thermoeconomic approach of Power, cooling and heating

Muhammed Arslan [a], Ceyhun Yılmaz [b,*]

[a] Afyon Kocatepe University, Çay Vocational School, Department of Motor Vehicles and Transportation Technologies, Afyonkarahisar
[b] Afyon Kocatepe University, Technology Faculty, Mechanical Engineering Department, Afyonkarahisar

ARTICLE INFO

Keywords:
Biogas plant
Heating and cooling
Optimization
Thermodynamic
Thermoeconomic

ABSTRACT

This study modeled and analyzed transforming an operational biogas power plant into a trigeneration system with power, cooling, and heating. In this context, the energy, exergy, and optimum unit energy costs of this trigeneration system's power, cooling, and heating are investigated. The transformation of the clean energy potential of Afyonkarahisar city as biogas into power is investigated and analyzed by realizing it on an established biogas power plant. The high-temperature exhaust gases from the power unit (PU) are directed to the generator of an absorption cooling system, operating the cooling unit (CU). Exhaust gases from the generator, which are still hot, start a heating unit (HU) for space heating and are released into the atmosphere. As a result of the optimization, The energy efficiency, exergy efficiency, fuel consumption, and unit electricity cost of the existing power plant are 39.54%, 34.65%, 0.3161 kg/s, and 0.042 $/kWh. By integrating the optimized cooling unit to power unit, energy efficiency, exergy efficiency, and unit cooling cost of the plant were 54.2%, 43.39%, and 0.0352 $/kWh. Finally, with the integration of the heating unit to the plant, energy efficiency, exergy efficiency, and unit heating cost of the plant were 74.2%, 50.14%, and 0.0178 $/kWh, respectively.

1. Introduction

People's energy demands have recently increased with economic, social, and technological developments. However, the increase in world energy demand is much higher than the increase in world population. In 2020, more than 87% of the world's energy demand was met by energy resources such as coal, crude oil, natural gas, and uranium. Today, these fuels cause climate change and the release of greenhouse gases. Although both primary energy and carbon emissions have decreased at their fastest rates in 2020 since the second world war, it is known that this is due to the dramatic impact of Covid-19 on the energy markets [1,2]. In the face of these ongoing problems, investigate energy production from sustainable and renewable sources [3]. Among renewable energy technologies, combining biomass energy with a fuel cell cogeneration system is one of the most attractive options that can generate sustainable power and, at the same time, reduce energy consumption and negative environmental impacts. Biomass has recently attracted great interest as an alternative to fossil fuels due to its widespread availability, near-zero CO_2/SO_2 emissions, and low cost compared to other energy sources [4]. The unique feature that distinguishes bioenergy from renewable energy types is storable. It plays an essential role in supplying energy needs where other types of energy are insufficient or limited [5].

Biogas, obtained from sustainable and renewable resources, is one of the most important members of the clean fuels family. Although it is rich in carbon, it is not a fossil fuel [6–7]. The advantages are low weed seed volume, fertilizer, odor, and pathogens, providing jobs in rural areas, and reducing emissions [8]. Biogas is a renewable energy source produced by decomposing organic materials (raw materials) under controlled temperature in a process known as anaerobic digestion in an oxygen-free environment [9]. Organic materials can be manure, food waste, industrial waste, and sewage sludge [10]. Another striking aspect of biogas is its use in cogeneration, and polygeneration systems can improve usage prices. Combine cooling, heating, and power generation (trigeneration) systems, briefly called CCHP, supply different energy types such as cooling, heating, power, and their total efficiencies are between 70% and 85% [11]. Exhaust gas is not only used for heating; it is also used for cooling in the LiBr absorption cooling system, which is the most popular choice due to its availability and technological

* Corresponding authors.
E-mail address: ceyhunyilmaz@aku.edu.tr (C. Yılmaz).

https://doi.org/10.1016/j.fuel.2022.124779
Received 5 April 2022; Received in revised form 17 May 2022; Accepted 2 June 2022
Available online 10 June 2022

Nomenclature

Symbols

AFR	Air Fuel Ratio
c	Unit Flow Cost Ratio [$/kWh]
C	Carbon
CC	Combustion Chamber
C_k	Equipment Purchase Cost [$]
$\dot{C}$	Exergy Cost Ratio [$/h]
CHP	Combined Heating and Power
CCHP	Combined Cooling Heating and Power
CH_4	Methane
CO_2	Carbon Dioxide
COP	Coefficient of Performance
CRF	Capital Recovery Factor
EES	Engineering Equation Solver
ex	Specific Exergy [kj/kg]
$\dot{E}x$	Exergy [kW]
Fr	Fraction [%]
h	Spesific Entalphy [kJ/kg]
HE	Heat Exchanger
HV	Heat Value [kJ/kg]
H_2O	Water
i	Interest Rate [%]
LiBr	Lithium Bromide
$\dot{m}$	Mass Flow Rate [kg/s]
N	Working Life [year]
N/N_2	Nitrogen
NH_3	Ammonia
O_2	Oxygen
OFC	Organic Flash Cycle
OMCF	Operation and Maintenance Correction Factor
ORC	Organic Rankine Cycle
P	Pressure [kPa]
pH	Potential of Hydrogen
$\dot{Q}$	Thermal Power [kW]
r_p	Rise of Pressure
s	Spesific Entropy [kJ/kgK]
SO_2	Sulfur Dioxide
SOFC	Solid Oxide Fuel Cell
ST	Solar Thermal
t	Operating Time [h]
T	Temperature [K or ℃]
$\dot{W}$	Power [kW]
$\dot{Z}_k$	Total Cost Ratio ($/h)

Subscripts

ch	Chemical
Des	Destruction
elec	Electric
F	Fuel
isen	Isentropic
k	th component
P	Product
rev	Reversible

Greek Symbols

η	First Law Efficiency
η_{II}	Second Law Efficiency
$	United State Dollars
$\sum$	Sum of Array

maturity. The CCHP systems in a home and industrial use play an important role in higher energy efficiency. In addition, these plants have lower emissions and energy consumption than conventional systems [12–14]. Many technologies are considered when designing the CCHP systems. The high-performance fuel cell's ability to branch and distribute electricity, quiet operation and environmental friendliness make it among the ideal electricity generation technologies in the CCHP systems [15]. However, internal combustion engines are preferred among small-scale solutions because of their wide availability, technological maturity, and load flexibility. In addition, the CCHP system, which includes different systems, requires much equipment and therefore capital; however, a biomass-based and small-scale CCHP system will increase self-sufficiency and reduce the ecological footprint. It will also provide long-term economic benefits with appropriate equipment selection and optimum sizing [13].

Many different types of studies are currently being carried out on CCHP systems driven by biogas. Some of them are: Su et al. (2018) presented a CCHP system with synthetic use of biogas and solar energy to facilitate fossil fuel energy consumption and increase the efficiency of biogas use. The analysis results showed that the synthetic use of biogas and solar energy reduces the annual electricity production by 8.7%, the energy used in cooling by 2.57%, the natural gas consumption by 8.66%, and the CO_2 footprint 8.2% compared to that of the reference systems [16]. Parikhani et al. (2020) investigated a CCHP system driven by a low-temperature heat source, a modified version of the Kalina cycle, from a thermodynamic and thermoeconomic point of view. As a result of the analysis, they obtained 49.83% energy efficiency, 27.68% exergy efficiency, and 198.3 $/GJ total unit product cost [17]. Peng et al. (2020) proposed a CCHP system model with solid oxide fuel cells (SOFC) and investigated the effect of fuel and oxidant flow rates on performance. The highest solid oxide fuel cell efficiency in the model was obtained as 38.57%, with fuel and oxidant flow rates of 89 and 1100 kg mol/h, respectively. In addition, the highest power produced by SOFC was 7864.6 kW, with fuel and oxidant flow rates of 93 and 1140 kg mol/h, respectively [18]. Wegener et al. (2021) proposed a dynamic model for a small-scale CCHP system based on the gasification of woody biomass species. The model also considered the effects of the chemical composition of the biomass and ambient temperatures on the exergy performance of the components. Analysis results showed that small-scale CCHP systems operate at higher exergy efficiency than large-scale CCHP systems [13]. Wei et al. (2021) proposed an optimized model to minimize the annual cost of a fuel cell-driven CCHP system and maximize economic efficiency. As a result of the optimization, a reduction in greenhouse gas of 4480 kg per year, exergy efficiency of 55.76%, and annual cost of 24,800 $ was obtained [15]. Ghamari et al. (2021) designed a CCHP system to supply a hotel's heating, cooling, electricity, and freshwater needs. They examined the effects of two types of equipment, diesel engine and gas turbine, on the annual cost to generate heat and power. As a result of the analysis, it was observed that the annual cost of with colloidal fouling, without colloidal fouling and thermal vapor compression very effective desalination CCHP systems of the diesel engine decreased by 9.66%, 1.8%, and 11.68%, respectively, compared to the gas turbine [14]. Aghaei and Saray (2021) proposed and optimized a CCHP system for a dairy factory. The proposed system has 20% electricity efficiency and a coefficient of performance (COP) higher than 1.2. As a result of the optimization, the fuel energy saving rate and CO_2 emission reduction rate of the CCHP system was approximately 45%, and the annual total cost savings rate was 37% [19]. Ai et al. (2022) designed a CCHP – solar thermal (ST) – organic flash cycle (OFC) system combining a ST input system and a regenerative OFC system and compared it thermodynamically with the conventional CCHP and CCHP – ST – organic rankine cycle (ORC) system. Analysis

results showed that CCHP – ST – OFC system provided 4.7 kW and 19.3 kW higher electricity and heat supply, respectively than CCHP – ST – ORC system. In addition, it was observed that the primary energy ratio and exergy efficiency of the CCHP - ST - OFC system were 53.1% and 38.7%, respectively, and it reduced natural gas consumption by 9% compared to CCHP - ST - ORC system [20].

This study has carried out the modeling and analysis of the transformation of an operational biogas power plant into a trigeneration system with power, cooling, and heating. In this context, the energy, exergy, and optimum unit energy costs of the power, cooling, and heating produced in this trigeneration system are investigated. In this study, the transformation of the clean energy potential of Afyonkarahisar province as biogas into power are investigated and analyzed by realizing it on an established biogas power plant. In addition, the combustion products in the Afyon Biogas Power Plant are converted into an efficient agricultural fertilizer. As a result of biogas combustion in the power plant, fertilizer, which is harmless to the environment and entirely beneficial, is produced [21]. This plant is financially supported by the European Union's support within the scope of its targets for reducing emissions such as CO_2 emissions.

In the presented study, a thermodynamic and thermoecononmic design and performance evaluation was made for a biogas power plant operating in Afyonkarahisar, Turkey, and the heating–cooling system was integrated into this plant using current data. Power, heating, and cooling system are modeled and combined by optimizing the biogas power plant. Optimization studies were performed for the thermodynamic analysis and design of the system and the optimum working conditions. The designed system is a feasibility study to provide clean energy for Afyonkarahisar city. In this context, the authorities presented the study, and innovative and useful research was conducted to increase the feasibility and energy efficiency of the existing power plant. The reason for making detailed computer simulations in Aspen Plus program in this study is to propose a real-time dynamic model of the system. The numerical analysis was only performed in the Engineering Equation Solver (EES). With the Aspen Plus program, detailed energy and economic analysis of the system was possible. For this reason, two different simulations were given, and it was seen that the results were compatible with each other.

The energy production process from biomass consists of 4 stages: a collection of biomass, preliminary, energy production, and energy use. This study focused on energy production and energy use [22]. This study performed a thermodynamic and thermoeconomic analysis of a biogas power plant with a net power capacity of 4000 kW. CCHP system consists of the power, heating, and cooling units. First of all, the power unit is optimized. Power unit optimization aims to achieve the same output power more efficiently with less fuel consumption than increasing net output power. Then the heating and cooling units are modeled and optimized. Thermodynamic and thermoeconomic optimization aims to improve thermodynamic performance and unit costs. According to EES results, parametric optimization was performed in the EES program, and the plant was modeled in the Aspen Plus program. The data obtained in both software are compatible with almost absolute accuracy. Also, the transfer of energy from exhaust gas in heating and cooling units makes the exhaust gas less harmful. So, optimization and integration processes provide environmental benefits and thermodynamic and thermoeconomic improvements.

2. Working principle of combined heat and power system

It proposed biogas energy for power, cooling, and heating production and constructed a model for accomplishing such a task. This section describes the Combine cooling, heating, and power generation model. Basic definitions and working principles for the thermodynamics of the model are expressed.

Since most of the raw material of the power plant in Afyonkarahisar is chicken manure, the composition of the produced biogas is assumed as 60% CH_4 – 40% CO_2. Biogas is purified from undesirable components such as hydrogen sulfide, ammonia, water, and nitrogen, released due to its production before the combustion event [21]. In traditional most cooling units, the compressor powered by an electric motor is used. The refrigerant produces cooling in a mechanical evaporation compression system by evaporating at low pressure. Then, it is compressed to higher pressure in a mechanical compressor and condensed in a condenser. On the other hand, Absorption coolers act according to the principle of separation of the working fluid in solution when heated. It produces cooling at low pressure and temperature in the evaporator, similar to the working principle of an electrically powered compressor. Nevertheless, the pump is preferred to move the working fluid more efficiently and provide pressure change in the system. The pump requires much less electricity than the compressor, and therefore absorption cooling systems are also of scientific and professional interest. So, as the cooling system, the absorption cooling system was chosen instead of the mechanical compressor cooling system in this study. In absorption cooling systems, two types of working fluids are used as LiBr – H_2O if the generator temperature is 76 – 99 ℃ and NH_3 – H_2O if 95 – 120 ℃. So, in this study, LiBr – H_2O was chosen as the working fluid, as a medium temperature has simultaneous positive effects on energy and exergy performance and exergoeconomic parameters and the generator temperature is 93 ℃ [11,23].

The produced biogas performs combustion in the combustion chamber with the air compressed in the compressor and heated in the preheater. The high-energy exhaust gas released makes the gas turbine runs to generate 4000 kW of net electricity output. The exhaust gases leaving the turbine still have high energy, and some of it heats the fresh air charge in the preheater. Then, the waste exhaust gas comes to the generator of the cooling cycle instead of being thrown into the atmosphere, driving the LiBr absorption cooling system. After the generator, LiBr is separated from H_2O by the heat. The heated water is cooled at constant pressure in the condenser and expands in the expansion valve. The evaporator performs the cooling process by cooling the space cooling water.

Meanwhile, LiBr transfers some energy to the LiBr – H_2O solution by passing through the regenerator. It then expands in the expansion valve and re-forms the mixture with the heated water in the absorber. In the meantime, the solution is cooled to make the absorption process more efficient. The cooling cycle pump pumps the LiBr – H_2O solution through the regenerator to the generator, and the cycle is complete. In this way, the hot water coming to the evaporator from the place to be cooled is circulated for cooling.

On the other hand, the gas exhaust gas still has high energy, although some of its energy has been transferred to the cooling cycle. Therefore, after the generator, the high-energy exhaust gas is emitted into the atmosphere after heating the water in the heat exchanger. Water, which is the working fluid of the heating cycle, is circulated between the space to be heated and the heat exchanger. The schematic view of the designed CCHP system is given in Fig. 1.

Some numerical values of the CCHP system are given in Table 1. Information of the plant's 4000 kW net output power is available on the plant's current status. Efficiency information is the average value of the efficiencies of types of equipment in the market. The high heat value of the biogas was also calculated in the EES by taking into account the high heat values of gases in the biogas composition.

Thermodynamic assumptions in the analysis are following [25,26]:

- Pressure drop during the flow of the working fluid through pipes or components such as heat exchangers can be neglected [27].
- There is no leakage in pipes connecting system components.
- All compression and expansion processes are quasi-equilibrium.
- Flow rates are steady.
- The values have been referenced as standard chemical exergy.
- Heat loss of the combustion chamber (CC) has been assumed as 2% ($\eta_{cc} = 98\%$) [28].

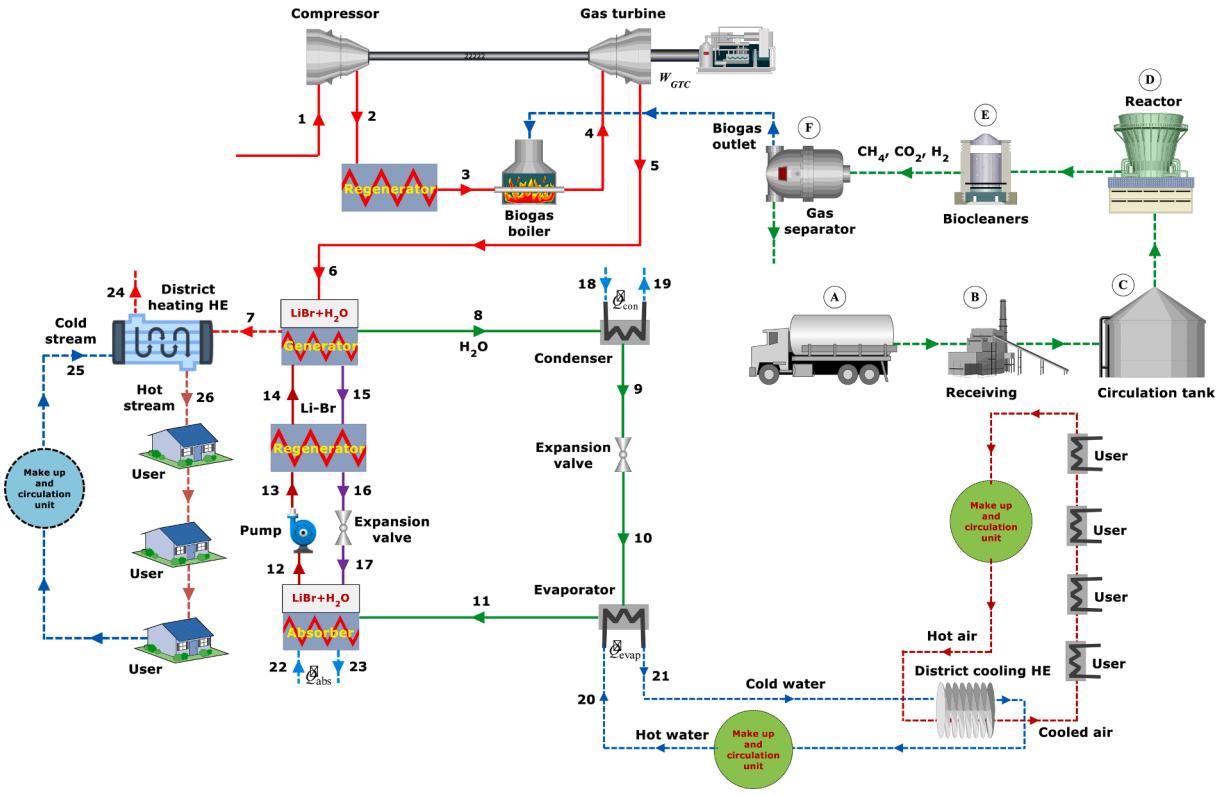

Fig. 1. Schematic view of the designed the Combine Cooling, Heating and Power (CCHP) system.

Table 1
Some numerical values of CCHP system [21,24].

Property	Value
Net electricity output power of power unit	4000 kW
Heat value of biogas (HV)	32000 kJ/kg
Atmospheric conditions	100 kPa and 300 K
Air Fule Ratio (AFR)	66.64
Pressure ratio (r_p)	8
Biogas mass flow rate (kg/s)	0.4797
$\eta_{isen.,\ compressor}$	85%
$\eta_{preheater}$	80%
$\eta_{isen.,\ turbine}$	85%
$\eta_{regenerato\ r}$	70%
$\eta_{isen.,\ pump}$	85%
$\eta_{electric\ generator}$	98%

- The properties of inlet and outlet gases in combustion are real gases properties.
- It has been assumed that combustion is complete combustion.
- Components of air entering to combustion chamber have been assumed as O_2 – 21% and N_2 – 79%.

3. Thermodynamic analysis

Energy and exergy calculations are necessary to evaluate the performance of the existing power plant and CCHP system in terms of thermodynamics. Exergy analysis is required to determine the irreversibility of plants and equipment with high irreversibility. The exergy data obtained are also used in the economic analysis of the system. In this way, diagnosis and improvement can be made in thermodynamics and thermoeconomics [29]. The thermodynamic analysis is performed using the steady-state thermodynamic values and the equations below.

For compressor,

$$\eta_{isen.,comp.} = \frac{h_{s2} - h_1}{h_2 - h_1} \tag{1}$$

$$\dot{W}_{comp.} = \dot{m}_1(h_2 - h_1) \tag{2}$$

$$\dot{W}_{rev.,comp.} = \dot{m}_1(ex_2 - ex_1) \tag{3}$$

$$\dot{E}x_{Des.,comp.} = \dot{W}_{comp.} - \dot{W}_{rev.,comp.} \tag{4}$$

for preheater,

$$\eta_{preheater} = \frac{h_3 - h_2}{h_5 - h_2} \tag{5}$$

$$\dot{E}x_{F,preheater} = \dot{m}_5(ex_5 - ex_6) \tag{6}$$

$$\dot{E}x_{P,preheater} = \dot{m}_2(ex_3 - ex_2) \tag{7}$$

$$\dot{E}x_{Des.,preheater} = \dot{E}x_{F,preheater} - \dot{E}x_{P,preheater} \tag{8}$$

for combustion chamber,

$$\left(\dot{m}_3 h_3 + \dot{m}_{biogas} HV_{biogas}\right)\eta_{CC} = \dot{m}_4 h_4 \tag{9}$$

$$\dot{E}x_{F,CC} = \dot{m}_{biogas} ex_{ch.,biogas} \tag{10}$$

$$\dot{E}x_{P,CC} = \dot{m}_4 ex_4 - \dot{m}_3 ex_3 \tag{11}$$

$$\dot{E}x_{Des.,CC} = \dot{E}x_{F,CC} - \dot{E}x_{P,CC} \tag{12}$$

for turbine,

$$\eta_{isen.,turb.} = \frac{h_4 - h_5}{h_4 - h_{s5}} \tag{13}$$

$$\dot{W}_{turb.} = \dot{m}_4(h_4 - h_5) \tag{14}$$

$$\dot{W}_{rev.,turb.} = \dot{m}_4(ex_4 - ex_5) \quad (15)$$

$$\dot{E}x_{Des.,turb.} = \dot{W}_{rev.,turb.} - \dot{W}_{turb.} \quad (16)$$

for generator,

$$\dot{m}_6(h_6 - h_7) = \dot{m}_8 h_8 + \dot{m}_{15} h_{15} - \dot{m}_{14} h_{14} \quad (17)$$

$$\dot{E}x_{P,gen.} = \dot{m}_8 ex_8 + \dot{m}_{15} ex_{15} - \dot{m}_{14} ex_{14} \quad (18)$$

$$\dot{E}x_{F,gen.} = \dot{m}_6(ex_6 - ex_7) \quad (19)$$

$$\dot{E}x_{Des.,gen.} = \dot{E}x_{F,gen.} - \dot{E}x_{P,gen.} \quad (20)$$

for condenser,

$$\dot{m}_8(h_8 - h_9) = \dot{m}_{19}(h_{19} - h_{18}) \quad (21)$$

$$\dot{E}x_{P,cond.} = \dot{m}_{18}(ex_{19} - ex_{18}) \quad (22)$$

$$\dot{E}x_{F,cond.} = \dot{m}_8(ex_8 - ex_9) \quad (23)$$

$$\dot{E}x_{Des.,cond.} = \dot{E}x_{F,cond.} - \dot{E}x_{P,cond.} \quad (24)$$

for expansion valve through in which water circulates,

$$h_9 \cong h_{10} \quad (25)$$

$$\dot{E}x_{P,exp.val.} = \dot{m}_{10} ex_{10} \quad (26)$$

$$\dot{E}x_{F,exp.val.} = \dot{m}_9 ex_9 \quad (27)$$

$$\dot{E}x_{Des.,exp.val.} = \dot{E}x_{F,exp.val.} - \dot{E}x_{P,exp.val.} \quad (28)$$

for evaporator,

$$\dot{m}_{10}(h_{11} - h_{10}) = \dot{m}_{20}(h_{20} - h_{21}) \quad (29)$$

$$\dot{E}x_{P,evap.} = \dot{m}_{10}(ex_{11} - ex_{10}) \quad (30)$$

$$\dot{E}x_{F,evap.} = \dot{m}_{20}(ex_{20} - ex_{21}) \quad (31)$$

$$\dot{E}x_{Des.,evap.} = \dot{E}x_{F,evap.} - \dot{E}x_{P,evap.} \quad (32)$$

for absorber,

$$\dot{m}_{12} h_{12} + \dot{m}_{23} h_{23} = \dot{m}_{11} h_{11} + \dot{m}_{17} h_{17} + \dot{m}_{22} h_{22} \quad (33)$$

$$\dot{E}x_{P,abs.} = \dot{m}_{23} ex_{23} - \dot{m}_{12} ex_{12} \quad (34)$$

$$\dot{E}x_{F,abs.} = \dot{m}_{11} ex_{11} + \dot{m}_{17} ex_{17} - \dot{m}_{12} ex_{12} \quad (35)$$

$$\dot{E}x_{Des.,abs.} = \dot{E}x_{F,abs.} - \dot{E}x_{P,abs.} \quad (36)$$

for regenerator,

$$\eta_{reg.} = \frac{h_{15} - h_{16}}{h_{15} - h_{13}} \quad (37)$$

$$\dot{E}x_{P,reg.} = \dot{m}_{13}(ex_{14} - ex_{13}) \quad (38)$$

$$\dot{E}x_{F,reg.} = \dot{m}_{15}(ex_{15} - ex_{16}) \quad (39)$$

$$\dot{E}x_{Des.,reg.} = \dot{E}x_{F,reg.} - \dot{E}x_{P,reg.} \quad (40)$$

for expansion valve through which LiBr circulates,

$$h_{16} \cong h_{17} \quad (41)$$

$$\dot{E}x_{P,exp.val.} = \dot{m}_{17} ex_{17} \quad (42)$$

$$\dot{E}x_{F,exp.val.} = \dot{m}_{16} ex_{16} \quad (43)$$

$$\dot{E}x_{Des.,exp.val.} = \dot{E}x_{F,exp.val.} - \dot{E}x_{P,exp.val.} \quad (44)$$

for pump,

$$h_{12} \cong h_{13} \quad (45)$$

$$\dot{E}x_{P,pump} = \dot{W}_{rev.,pump} \quad (46)$$

$$\dot{E}x_{F,pump} = \dot{W}_{pump} \quad (47)$$

$$\dot{E}x_{Des.,pump} = \dot{E}x_{F,pump} - \dot{E}x_{P,pump} \quad (48)$$

for heat exchanger (HE),

$$\dot{m}_7 h_7 + \dot{m}_{25} h_{25} = \dot{m}_{24} h_{24} + \dot{m}_{26} h_{26} \quad (49)$$

$$\dot{E}x_{P,HE.} = \dot{m}_{25}(ex_{26} - ex_{25}) \quad (50)$$

$$\dot{E}x_{F,HE.} = \dot{m}_7(ex_7 - ex_{24}) \quad (51)$$

$$\dot{E}x_{Des.,HE.} = \dot{E}x_{F,HE.} - \dot{E}x_{P,HE.} \quad (52)$$

The above equations are used to evaluate the system thermodynamically. The COP of the cooling system is calculated by the ratio of the heat transferred to the refrigerant in the evaporator to the heat entering the cooling system in the generator:

$$COP = \frac{\dot{Q}_{evap.}}{\dot{Q}_{gen.}} \quad (53)$$

The energy and exergy efficiency of the CCHP system are as follows, respectively.

$$\eta_{CCHP} = \frac{\dot{Q}_{elec.} + \dot{Q}_{evap.} + \dot{Q}_{HE.}}{\dot{m}_{biogas} HV_{biogas}} \quad (54)$$

$$\eta_{II,CCHP} = \frac{\dot{Q}_{elec.} + \dot{E}x_{Cooling} + \dot{E}x_{Heating}}{\dot{E}x_{ch,biogas}} \quad (55)$$

$$\dot{E}x_{Cooling} = \left(1 - \frac{T_0}{T}\right)\dot{Q}_{Cooling,in} \quad (56)$$

$$\dot{E}x_{Heating} = \left(1 - \frac{T_0}{T}\right)\dot{Q}_{Heating,in} \quad (57)$$

The ratio of the exergy destruction of each equipment to the total exergy destruction is used to see the highest exergy destruction in the plant.

$$Fr_{Des.Ex_k} = \frac{\dot{E}x_{Des.,k}}{\sum_{n=1}\dot{E}x_{Des.,n}} \quad (58)$$

4. Thermoeconomic analysis

Thermoeconomic analysis calculates the unit costs of electricity, heating, and cooling in the modeled system and the exergy costs in each case. The aim is to decide whether the heating, cooling, and electricity power produced is expensive or cheap. In order to obtain unit costs, it is necessary to calculate many variables such as equipment purchase cost (C_k), operation and maintenance correction factor (OMCF), capital recovery factor (CRF), and unit flow cost ratio (c). Equipment purchase costs are taken from Aspen Plus software, which contains up-to-date equipment costs. OMCF = 1.06, interest rate (i) = 10%, and N = 20 to be considered as the working life of the power plant in years [28]:

$$CRF = \frac{i(i+1)^N}{(i+1)^N - 1} \quad (59)$$

The CRF equation calculates it. In this case, the total cost ratio of each equipment ($\dot{Z}_k$) is:

$$\dot{Z}_k = C_k \frac{CRF}{t} OMCF \quad (60)$$

Where t is the operating time of the plant in hours per year:

$$t = 365 \times 24 \times 0.9 \tag{61}$$

In this case, the unit electricity cost for the power unit is calculated with the following equations:

$$c_{elec.}\dot{W}_{comp.} + c_1\dot{E}x_1 + \dot{Z}_{comp.} = c_2\dot{E}x_2 \tag{62}$$

$$c_2\dot{E}x_2 + c_5\dot{E}x_5 + \dot{Z}_{preheater} = c_3\dot{E}x_3 + c_6\dot{E}x_6 \tag{63}$$

$$c_3\dot{E}x_3 + c_{biogas}\dot{E}x_{ch.biogas} + \dot{Z}_{CC.} = c_4\dot{E}x_4 \tag{64}$$

$$c_4\dot{E}x_4 + \dot{Z}_{turb.} = c_5\dot{E}x_5 + c_{elec.}\dot{W}_{turb.} \tag{65}$$

The following equations are used to calculate the unit cooling cost:

$$c_6\dot{E}x_6 + c_{14}\dot{E}x_{14} + \dot{Z}_{gen.} = c_7\dot{E}x_7 + c_8\dot{E}x_8 + c_{15}\dot{E}x_{15} \tag{66}$$

$$c_8\dot{E}x_8 + c_{18}\dot{E}x_{18} + \dot{Z}_{cond.} = c_9\dot{E}x_9 + c_{19}\dot{E}x_{19} \tag{67}$$

$$c_9\dot{E}x_9 + \dot{Z}_{exp.val.} = c_{10}\dot{E}x_{10} \tag{68}$$

$$c_{10}\dot{E}x_{10} + c_{20}\dot{E}x_{20} + \dot{Z}_{evap.} = c_{11}\dot{E}x_{11} + c_{21}\dot{E}x_{21} \tag{69}$$

$$c_{11}\dot{E}x_{11} + c_{17}\dot{E}x_{17} + c_{22}\dot{E}x_{22} + \dot{Z}_{abs.} = c_{12}\dot{E}x_{12} + c_{23}\dot{E}x_{23} \tag{70}$$

$$c_{12}\dot{E}x_{12} + c_{elec.}\dot{W}_{pump} + \dot{Z}_{pump} = c_{13}\dot{E}x_{13} \tag{71}$$

$$c_{13}\dot{E}x_{13} + c_{15}\dot{E}x_{15} + \dot{Z}_{reg.} = c_{14}\dot{E}x_{14} + c_{16}\dot{E}x_{16} \tag{72}$$

$$c_{16}\dot{E}x_{16} + \dot{Z}_{exp.val.} = c_{17}\dot{E}x_{17} \tag{73}$$

$$c_{cooling} = c_{21} \tag{74}$$

The following equations are used to calculate the unit heating cost:

$$c_7\dot{E}x_7 + c_{25}\dot{E}x_{25} + \dot{Z}_{HE.} = c_{24}\dot{E}x_{24} + c_{26}\dot{E}x_{26} \tag{75}$$

$$c_{heating} = c_{26} \tag{76}$$

for the exergy cost ratio,

$$\dot{C}_k = c_k\dot{E}x_k \tag{77}$$

The total cost ratios of each equipments are calculated and given with equipment purchase costs in EES with data from Aspen Plus software and given in Table 2.

5. Results and discussions

5.1. Optimization and parametric study of the system

The thermoeconomic optimization procedure is applied using the genetic algorithm method to the model of this study. The objective is to minimize the unit costs of the composed system's products (electricity, cooling, and heating). The optimization approach is developed based on the cost-optimal exergetic efficiency obtained for a component isolated from the remaining system components. Optimization is performed based on thermoeconomic analysis. The effect of the component itself and the effects of all system components of a system should be taken into account. A parametric study was performed in the EES program. Although the "Genetic Method" method is slow, it is a method that can almost always find optimum global values. The parametric study results were confirmed by the "Genetic Method" [31]. The effects of the changes in the operational ranges of the input functions on output functions are investigated.

Input functions and operational ranges can be listed as follows: Input functions and ranges for power unit 60 ≤ Air fuel ratio (AFR) ≤ 80, 6 ≤ rise of pressure (r_p) ≤ 15; input functions and ranges for cooling unit 7 kPa ≤ cooling cycle high pressure ≤ 10 kPa, 0.7 kPa ≤ cooling cycle low pressure ≤ 1 kPa. The output functions are electricity cost, cooling and heating costs, energy efficiency, and exergy efficiency. The input values of AFR, r_p, cooling cycle high pressure and cooling cycle low pressure are 66.64, 8, 8.657 kPa and 0.8756 kPa, respectively.

Fig. 2 shows the effect of AFR on thermodynamic and thermoeconomic performance. According to the figure, the optimum AFR is 60. In terms of thermodynamics, an increase in AFR under normal conditions provides a performance improvement. However, this study aims not to increase the 4000 kW net output power but to obtain the same power more efficiently with less fuel consumption due to optimization. Achieving the same power with lower AFR means that performance has increased. Similarly, from a thermoeconomic point of view, the increase in AFR causes electricity to be produced more inefficiently and increases the cost. However, with the increase of AFR, the exhaust gas energy increases, and the heating and cooling units work more efficiently. This results in lower heating and cooling costs.

Fig. 3 shows the effect of r_p on thermodynamic and thermoeconomic performance for the power unit of the system. According to the figure, the optimum r_p is 6. r_p and AFR have similar effects on thermodynamic and thermoeconomic performance. As a result of optimization, reaching 4000 kW net output power with lower r_p means increased performance. An increase in r_p increases the cost of electricity and reduces heating and cooling costs. The efficient operation of the power unit that produces electricity reduces the energy of exhaust gas. This adversely affects the performance of the heating and cooling units.

In optimization of cooling cycle high pressure, it is seen that pressure has no significant effect on any output function. The increase in pressure only affected the cooling cost and slightly increased it. The optimum pressure was 7 kPa.

In optimization of cooling cycle low pressure, it is seen that pressure has no significant effect on any output function except cooling cost. An increase in pressure adversely affects cooling performance in the evaporator. So, cooling cost seriously increases. The optimum pressure was 0.7 kPa, and Fig. 4 shows the effect of cooling cycle low pressure on cooling cost.

Thermodynamic steady-state values obtained as a result of the optimization are given in Table 3. When we visited the plant, we obtained data about the thermodynamic operating conditions of the plant. The values in the table were obtained due to the optimization of these data and the integration of heating and cooling units. The values were then used in thermodynamic and thermoeconomic analysis.

Table 2
Total cost rate and equipment purchase cost of each equipments [30].

Equipment	$\dot{Z}$($/h)	Ck ($/h)
Absorber	6.444	300,000
Combustion Chamber	1.106	51,500
Condenser	6.444	300,000
Generator	6.444	300,000
Regenerator	6.444	300,000
Evaporator	0.4296	20,000
Expansion Valve (H_2O)	0.4296	20,000
Compressor	8.866	412,756
Turbine	7.223	336,246
Heat Exchanger	6.444	300,000
Preheater	0.7282	33,900
Pump	0.4403	20,500
Expansion Valve (LiBr)	0.4296	20,000

5.2. Thermodynamic analysis results

Biogas plants generally operate at high AFR values such as 60–100. The desired temperature T_4 determines excess air at the inlet of the gas turbine. Temperature T_4 is an important design variable that affects the entire system's performance. Before combustion, the AFR was set to about 60, and in this case, the mass flow rate of air and mass flow rate of

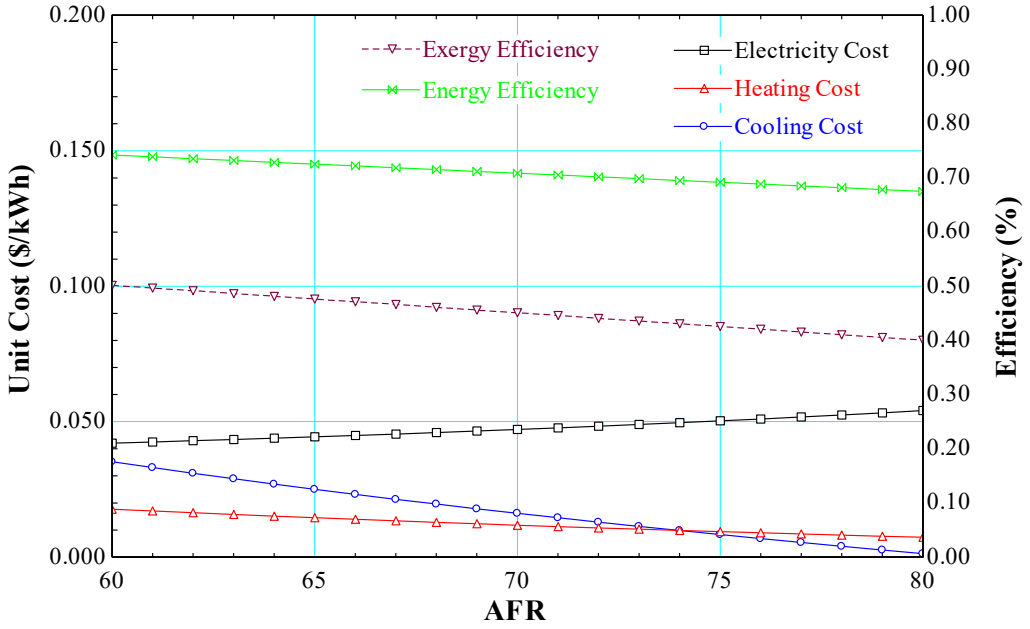

Fig. 2. Effect of AFR on thermodynamic and thermoeconomic performance.

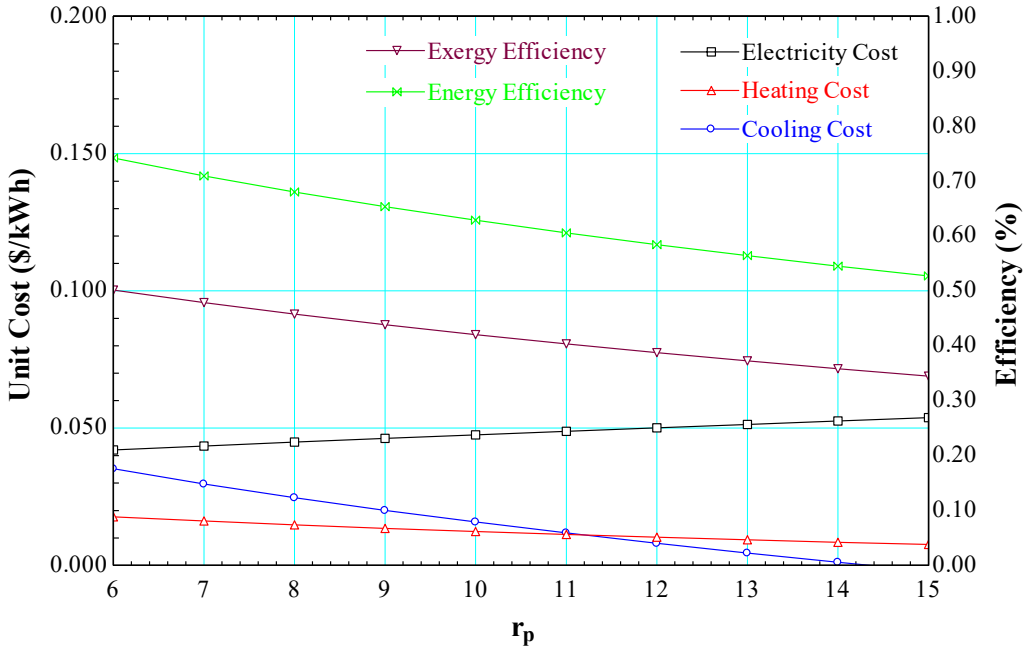

Fig. 3. Effect of r_p on thermodynamic and thermoeconomic performance.

biogas were calculated as 18.97 kg/h and 0.3161 kg/s, respectively. Exhaust gas components released from combustion are CO_2, H_2O, O_2, and N_2. The flow rates of LiBr and H_2O in the cooling unit were calculated as 7.393 kg/s and 0.6337 kg/s, respectively, and the COP value was 0.7208. Similarly, the flow rate of water, which is the working fluid of the heating unit, was determined as 24.08 kg/s.

Fig. 5 shows energy efficiencies of the current power unit, optimized power unit, optimized power unit + cooling unit, and optimized CCHP system. According to the figure, the efficiency of the plant increases by optimizing and integrating each unit into the power unit. In an optimized plant, the power released from combustion is 10,116 kW. In this case, the plant produces 4000 kW net electrical power, 1484 kW cooling power, and 2023 kW heating power. So, the efficiencies of the current power unit, optimized power unit, optimized power unit plus cooling unit, and optimized CCHP system is 26.49%, 39.54%, 54.2%, and 74.2%, respectively.

Fig. 6 shows exergy efficiencies of the current power unit, optimized power unit, optimized power unit plus cooling unit, and optimized CCHP system. Like in the energy graph, the exergy efficiency of the plant increases by optimizing and integrating each unit to plant. In an optimized plant, biogas, the chemical exergy of biogas is 11543 kW and represents exergy entering the plant. In this case, reversible cooling and heating powers are 1008 kW and 779.7 kW, respectively. So, exergy efficiencies of the current power unit, optimized power unit, optimized power unit plus cooling unit, and optimized CCHP are 23.22%, 34.65%, 43.39%, and 50.14%, respectively. Exergy efficiency has increased since

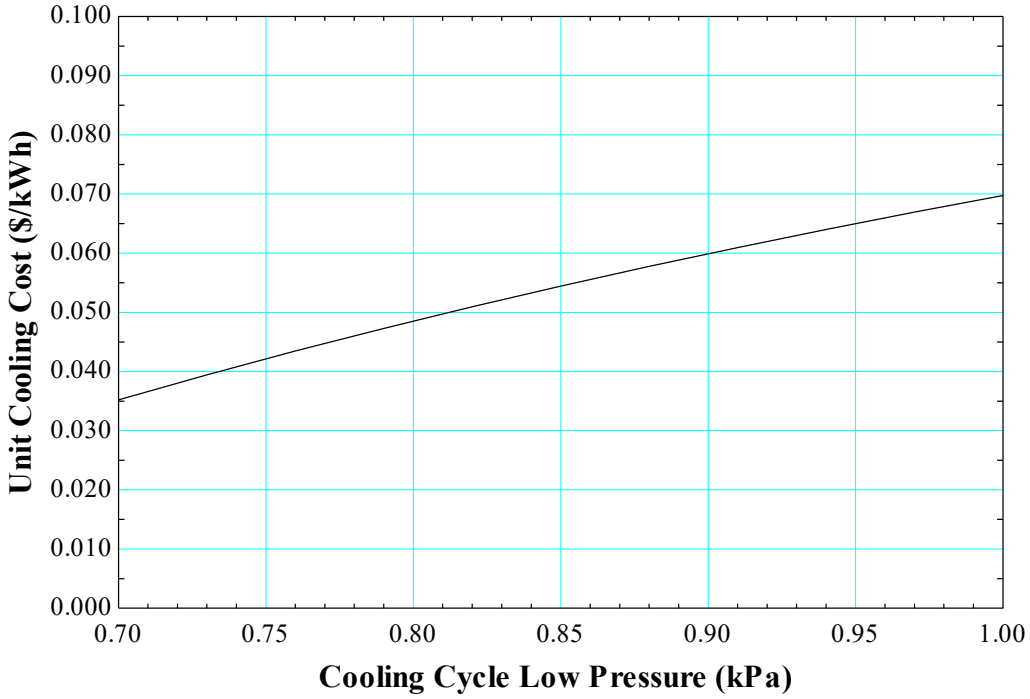

Fig. 4. Effect of cooling cycle low pressure on cooling cost.

Table 3
Steady state thermodynamic values for each states of the optimized CCHP system.

State	Fluid	T (K)	P (kPa)	$\dot{m}$(kg/s)	h (kJ/kg)	s (kJ/kgK)	Solution (%)	$\dot{E}x$(kW)
1	Air	300	100	18.97	300.4	5.706	–	0
2	Air	515.5	100	18.97	519.4	5.74	–	3956
3	Air	792.8	600	18.97	814.4	6.197	–	6952
4	Exh. gas	1211	600	19.28	1315	6.47	–	14,024
5	Exh. gas	849.4	100	19.28	888.1	6.575	–	5186
6	Exh. gas	588.2	100	19.28	598	6.167	–	1948
7	Exh. gas	488.2	100	19.28	491.2	5.968	–	1040
8	Water	366.3	7	0.6337	2675	8.579	–	77.79
9	Water	312.1	7	0.6337	163.4	0.559	–	0.8
10	Water	275	0.7	0.6337	163.4	0.594	–	0.87
11	Water	275	0.7	0.6337	2504	9.106	–	99.41
12	LiBr – H_2O	315.4	0.7	8.027	117.7	0.2468	59.5	425.9
13	LiBr – H_2O	315.4	7	8.027	117.7	0.2468	59.5	425.9
14	LiBr – H_2O	349.5	7	8.027	184	0.4463	59.5	481
15	LiBr	371.7	7	7.393	248.9	0.5273	64.6	760
16	LiBr	331.7	7	7.393	176.9	0.3198	64.6	668.2
17	LiBr	331.7	0.7	7.393	176.9	0.3198	64.6	630.1
18	Water	303	100	63.46	125.1	0.4347	–	4.603
19	Water	309	100	63.46	150.2	0.5166	–	46.27
20	Water	288	100	44.21	62.45	0.2223	–	45.4
21	Water	280	100	44.21	28.89	0.1041	–	129.1
22	Water	303	100	93.3	125.1	0.4347	–	6.768
23	Water	308	100	93.3	146	0.5031	–	54.73
24	Exh. gas	388.2	100	19.28	386.3	5.728	–	402.3
25	Water	343	100	24.08	292.4	0.9533	–	434
26	Water	363	100	24.08	376.4	1.191	–	796

exergy losses have been reduced as a result of optimization. Optimizing the power unit has increased exergy efficiency. In addition, the integration of heating and cooling units operating at lower temperatures than that of power unit has also increased exergy efficiency.

Component level exergy analysis is necessary to know which equipments have the highest destructions. Exergy destructions of each piece of equipment and their fractions in total exergy destruction of the CCHP system are given in Table 4. The table shows that the highest exergy destruction is in the combustion chamber due to finite temperature differences and thermal losses. Afterward, the highest exergy destructions are caused by fractions and heat transfer and belong to equipment such as turbine, generator, preheater, compressor, absorber.

Fig. 7 shows exergy flow and fractions of each component in exergy distribution. 11543 kW fuel exergy represents the exergy input of the power plant. The exergy losses in the power unit, heating unit, and cooling unit are indicated in italics in the figure and result in that total exergy reduces almost 60%. Here, it is seen that the main reason for the exergy losses is combustion chamber and, therefore, power unit.

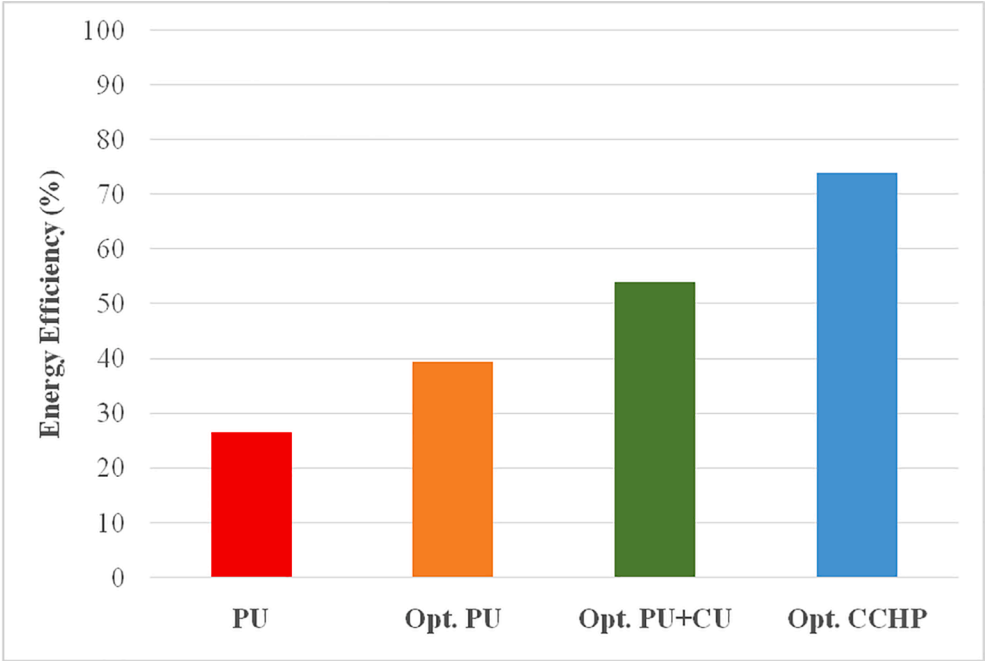

Fig. 5. Energy efficiencies of the current power unit, optimized power unit, optimized power unit plus cooling unit, and optimized CCHP system.

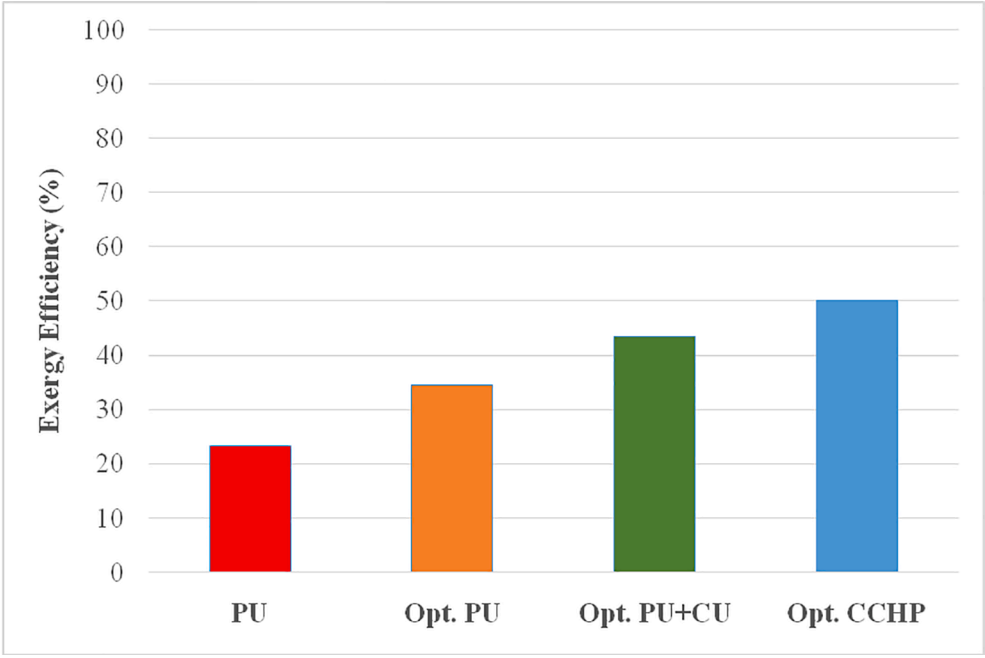

Fig. 6. Exergy efficiencies of the current power unit, optimized power unit, optimized power unit plus cooling unit, and optimized CCHP system.

5.3. Computer simulation of Combine Cooling, heating and power system

In this section, after the numerical analysis of the system, whose working principle and acceptances are given in Section 2, is made in the EES program, a dynamic simulation is made in the Aspen Plus program over the same assumptions and existing plant data. In particular, the design and model of the biogas digestion unit were developed here. It is not possible to model this part in the EES program. In the Aspen Plus program, energy and economic analysis can be made through the dynamic simulation of all model stages. The general results of the analysis are given in the figures. As can be seen, it is observed that the simulation results are also compatible with the EES analysis results.

Aspen Plus is a simulator leading chemical process in the market. It is also software that will allow the user to build a process model and then simulate it using complex calculations (models, equations, math calculations, regressions, etc.). It has many advantages, from designing new processess to improving current processess. Also, time-saving and accuracy are two of most attractive sides. In Fig. 8, the biogas production process in Aspen Plus is seen. The biomass received into the power plant is approximately 340 tons/day, and chicken manure constitutes 80% of the biomass. The biomass is first mixed with water, and the digestion process takes place in the reactor at 35 ℃. Biogas is released at the end of the digestion. Before the biogas is sent to the engine, it is purified from the unwanted components in its content. Thus, the biogas becomes

Table 4
Exergy destructions of each equipment and their fractions in total exergy destruction.

Equipment	Exergy Destruction	Fraction (%)
Absorber	255.6	3.68
Combustion Chamber	4471	64.41
Condenser	65.81	0.51
Generator	519.9	7.93
Regenerator	36.74	0.53
Evaporator	183.1	2.65
Compressor	196.3	2.82
Turbine	604.4	8.7
Heat Exchanger	273.8	3.94
Preheater	241.7	3.48
Pump	76.04	0.74
Expansion Valve (LiBr)	38.18	0.55
Expansion Valve (H_2O)	2.82	0.02
Total	**6941**	**100**

ready for combustion [30].

Fig. 9 shows electricity production in the power unit in the Aspen Plus software. Atmospheric air is compressed in the compressor and heated in the preheater. The air and produced biogas react in the combustion chamber and drive the turbine. The power produced in the turbine is 10727 kW, and the power required for the compressor is 6642 kW. In this case, 4085 kW net power is obtained. If it is assumed that an electrical generator operating with 98% efficiency in EES is also in Aspen Plus, the net electrical power produced will be 4003 kW. This value is almost the same as a result in EES. After the turbine, the exhaust gases arrive at the preheater to heat fresh air charge. It is then sent to a cooling unit to use waste energy [30].

Fig. 10 shows processes in cooling and heating units. The high-energy exhaust gas reaches the generator and transfers its energy to the LiBr-H_2O solution. In this way, LiBr and H_2O are separated. Then water takes 1481 kW of heat from space, cooling water in the evaporator. This value is perfectly compatible with 1484 kW of heat taken from space cooling water in the evaporator in EES. The exhaust gas leaving the generator reaches the heat exchanger and transfers its energy to space heating water. It is then released into the atmosphere. The 2023 kW heat transferred to heating water is the same as EES data. Finally, Fig. 11 shows the CCHP system in Aspen Plus software.

5.4. Thermoeconomic analysis results

Thermoeconomic equations and assumptions given in the thermoeconomic analysis section for thermoeconomic analysis are coded in EES. As a result of the analysis, CRF was calculated as 0.08718. Exergy, exergy costs, and unit electricity, heating, and cooling cost ratios for each cases are calculated using Aspen Plus software. The current economic datas are given in Table 5 [30]. As a result of the analysis and

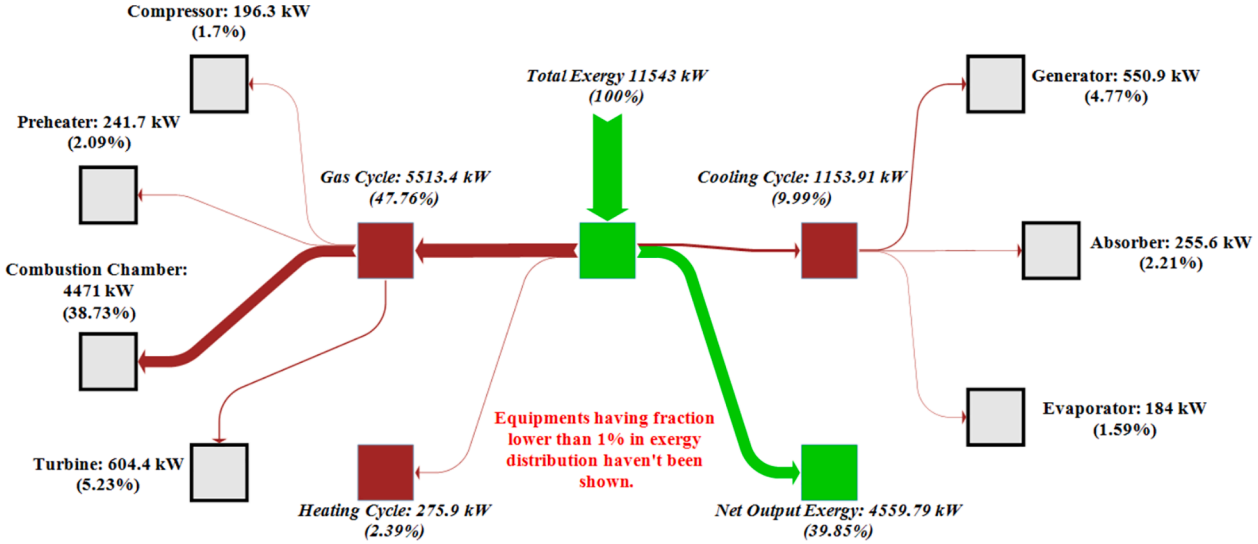

Fig. 7. Exergy flow and fractions of each component in exergy distribution.

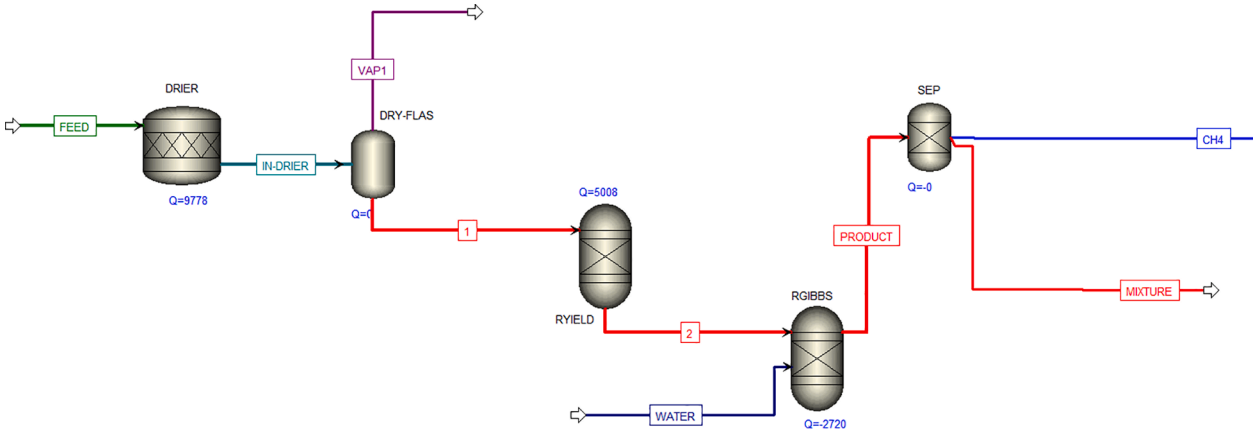

Fig. 8. The biogas production process in a computer simulation.

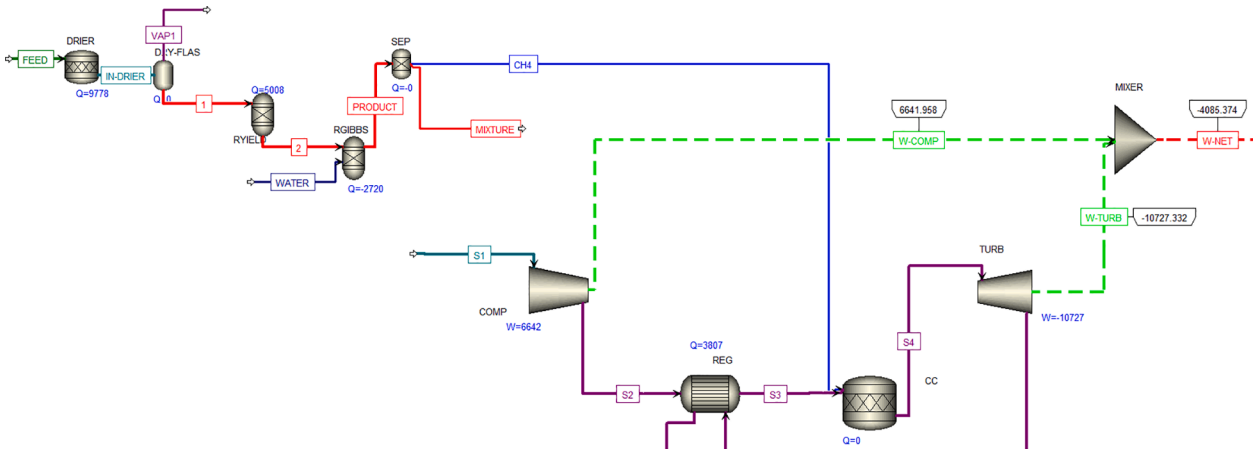

Fig. 9. Electricity production in the biogas power unit in a computer simulation.

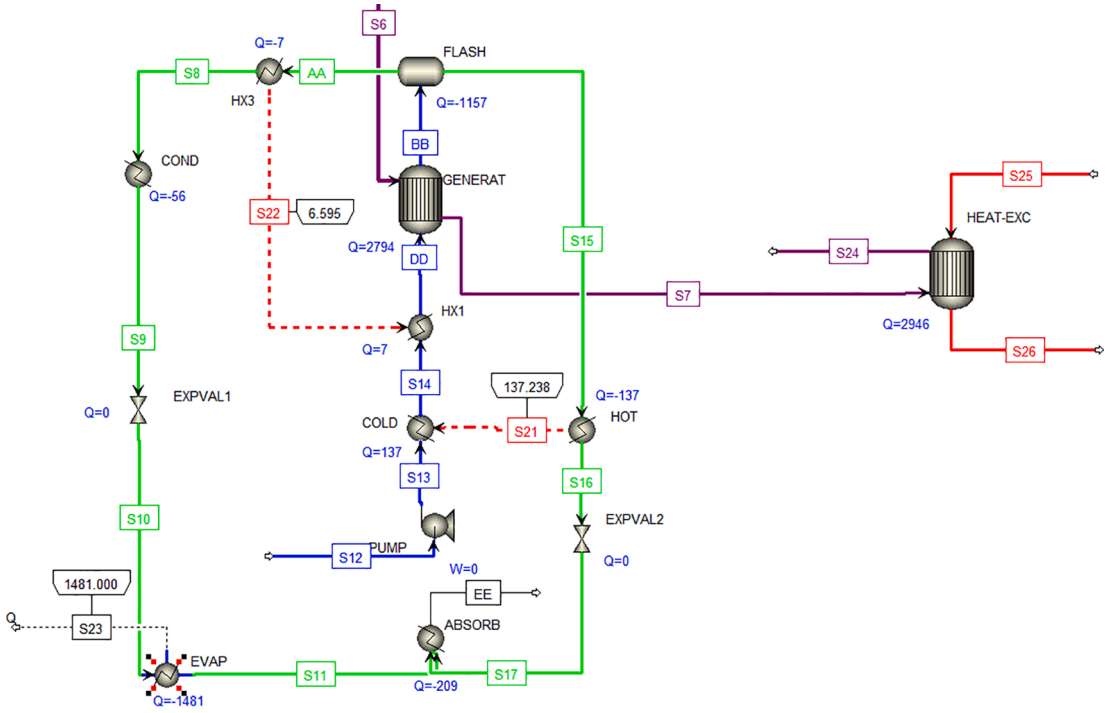

Fig. 10. Processes in cooling and heating units in a computer simulation.

optimization studies, the unit costs of electricity, cooling, and heating produced in the CCHP system are calculated as 0.042 $/kWh, 0.0352 $/kWh, and 0.0178 $/kWh, respectively. With the same biogas input, the cost figures of three different useful outputs to compete with the market show that the model is a viable and green light.

With this study, an important point has been added to the literature by considering the issue of using energy resources more efficiently and minimizing their environmental effects. Using waste heat in the developed model, heating and cooling using fossil resources will be done. The cooling and heating method from the clean electricity and waste heat produced by this study will reduce the use of fossil resources and reduce polluting environmental effects.

5.5. *Validation of proposed system*

In this section, an evaluation of the presented study in terms of energy end exergy efficiencies and product costs with combined systems in different studies is given in Table 6. The critical results of some studies on CCHP systems are given together with the presented study. The table evaluates and discusses thermodynamically energy and exergy efficiencies, thermoeconomic electricity, heating and cooling costs. According to the table, the presented study is at a better point both thermodynamically and thermoeconomically according to the references studies. It is understood that especially exergy efficiency is effective on unit costs.

6. Conclusion

In this study, the Combined Cooling, Heating, and Power (CCHP) system is thermodynamically and thermoeconomically optimized by integrating the heating and cooling units into a biogas power plant. Optimization aims to reduce the unit cost of electricity, heating, and cooling and increase energy and exergy efficiencies. Thermodynamic and thermoeconomic analysis is primarily performed at EES. Then, similar analyzes are performed in the Aspen Plus computer simulation environment. The results of the study are as follows:

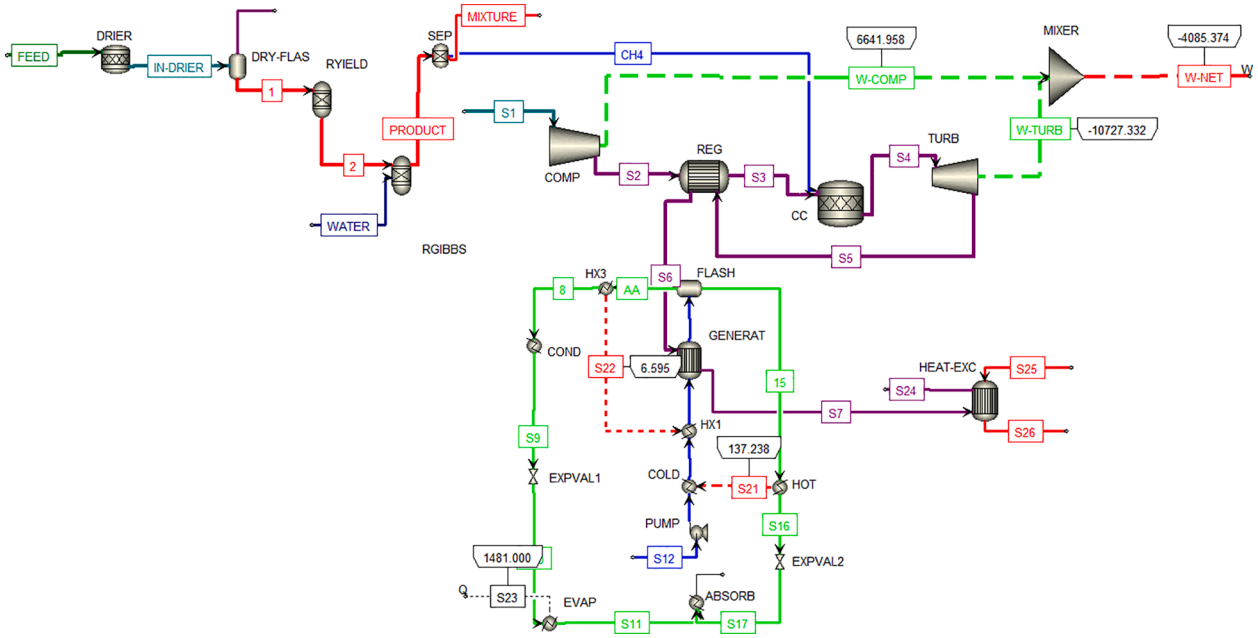

Fig. 11. CCHP system in a computer simulation.

Table 5
Exergy cost ratios and unit flow cost ratios for each states in the CCHP system.

State	c ($/GJ)	$\dot{C}$($/h)	State	c ($/GJ)	$\dot{C}$($/h)
1	0	0	14	0.0075	12.99
2	0.01289	183.6	15	−0.015	−41.05
3	0.01233	308.6	16	−0.015	−36.09
4	0.01066	538.2	17	−0.01572	−35.66
5	0.01066	199	18	0	0
6	0.01066	74.75	19	0.8622	143.6
7	0	0	20	0	0
8	0.4829	135.2	21	0.009777	4.543
9	−0.6739	−1.942	22	0	0
10	0.4829	−1.512	23	−0.222	−43.73
11	−0.01572	−5.626	24	0	0
12	0.0058	8.894	25	0.004917	7.725
13	0.0075	11.5	26	0.004917	14.17
Unit Costs ($/kWh)					
Electricity		Heating		Cooling	
0.042		0.0178		0.0352	

Table 6
Proposed system validation and comparisons with literature studies.

Referance studies	Efficiency (%)		Unit Costs ($/kWh)		
	Energy Efficiency	Exergy Efficiency	Electricity	Cooling	Heating
Ghiasirad et al. [32]	70.58	43.59	0.5627	0.2019	0.0573
Parikhani et al. [33]	49.83	27.68	1.08	0.6624	0.419
Ghaebi et al. [34]	84.01	43.92	0.0752	0.1634	0.041
Presented study	74.20	50.14	0.042	0.0352	0.0178

- The power unit of the current power plant produces 4000 kW of net electrical power with an energy efficiency of 26.49%, exergy efficiency of 23.22%, the fuel consumption of 0.4718 kg/s, and unit electricity cost of 0.0492 $/kWh. Optimization of the power unit aims to obtain the same power more efficiently by reducing fuel consumption rather than increasing net electrical power. Optimization reduces unit product costs by reducing exergic losses. As a result of the optimization, the power unit produces 4000 kW of net electrical power with 39.54% energy efficiency, 34.65% exergy efficiency, 0.3161 kg/s fuel consumption, and 0.042 $/kWh unit electricity cost. In order to benefit from the exhaust gas waste heat of the plant, heating, and cooling units were designed and integrated into the plant by optimizing. With the integration of an optimized cooling unit, the plant's energy efficiency was 54.2%, the exergy efficiency was 43.39%, and the unit cooling cost was 0.0352 $/kWh. Finally, with the integration of the heating unit, the energy efficiency was 74.2%, the exergy efficiency was 50.14%, and the unit heating cost was 0.0178 $/kWh.
- It has been seen in the thermoeconomic analysis that unit electricity cost in power unit optimization has the opposite character with unit heating and cooling costs. Improvements in the power unit reduce both unit electricity cost and exhaust gas energy. This will adversely affect the heating and cooling units, so these costs increase. As most power generation in the plant is electricity power, unit electricity cost is the focus of optimization.
- Optimization and integration positively affect the environment and thermodynamic and thermoeconomic improvement. After integration, exhaust gases with high energy are released with lower energy to the atmosphere. Therefore, the damage to the environment is reduced.
- Biogas composition of 60%, which is the energy source of the CCHP system, is methane. The high methane ratio increases the heating value of the fuel and thus the power plant's performance. In biogas production, pH, waste content, C/N ratio, and reactor temperature affect the methane ratio. Using lipids as waste, 25 – 30C/N ratio, 6.8 – 7.5 pH value, and high temperatures increase methane rate

Declaration of Competing Interest

The authors declare that they have no known competing financial interests or personal relationships that could have appeared to influence the work reported in this paper.

References

[1] Pereira JS, Riberio JB, Mendes R, Vaz GC, André JC. ORC based micro-cogeneration systems for residential application – A state of the art review and current challenges. Renew Sustain Energy Rev 2018;92:728–43.

[2] Petroleum B. Statistical Review of World Energy. 70th edition. www.bp.com. 2021.
[3] Rincón-Pérez J, Celis LB, Morales M, Alatriste-Mondragón F, Tapia-Rodríguez A, Razo-Flores E. Improvement of methane production at alkaline and neutral pH from anaerobic co-digestion of microalgal biomass and cheese whey. Biochem Eng J 2021;169:107972.
[4] Salehi A, Mousavi SM, Fasihfar A, Ravanbakhsh M. Energy, exergy, and environmental (3E) assessments of an integrated molten carbonate fuel cell (MCFC), Stirling engine and organic Rankine cycle (ORC) cogeneration system fed by a biomass-fueled gasifier. Int J Hydrogen Energy 2019;44(59):31488–505.
[5] Ohnmacht B, Lemmer A, Oechsner H, Kress P. Demand-oriented biogas production and biogas storage in digestate by flexibly feeding a full-scale biogas plant. Bioresour Technol 2021;332:125099.
[6] Abd Allah WE, Tawfik MA, Sagade AA, Gorjian S, Metwally KA, El-Shal H. Methane production enhancement of a family-scale biogas digester using cattle manure and corn stover under cold climates. Sustainable Energy Technol Assess 2021;45:101163.
[7] Abusoglu A, Tozlu A, Anvari-Moghaddam A. District heating and electricity production based on biogas produced from municipal WWTPs in Turkey: A comprehensive case study. Energy 2021;223:119904.
[8] Jarrar L, Ayadi O, Al Asfar J. Techno-economic Aspects of Electricity Generation from a Farm Based Biogas Plant. Journal of Sustainable Development of Energy, Water and Environment Systems 2020;8:476–92.
[9] Bedoić R, Dorotić H, Schneider DR, Ćućek L, Ćosić B, Pukšec T, et al. Synergy between feedstock gate fee and power-to-gas: An energy and economic analysis of renewable methane production in a biogas plant. Renewable Energy 2021;173:12–23.
[10] Scheutz C, Fredenslund AM. Total methane emission rates and losses from 23 biogas plants. Waste Manage 2019;97:38–46.
[11] Norani M, Deymi-Dashtebayaz M. Energy, exergy and exergoeconomic optimization of a proposed CCHP configuration under two different operating scenarios in a data center: Case study. J Cleaner Prod 2022;342:130971.
[12] Cao Y, Dhahad HA, Togun H, Abdollahi Haghghi M, Anqi AE, Farouk N, et al. Seasonal design and multi-objective optimization of a novel biogas-fueled cogeneration application. Int J Hydrogen Energy 2021;46(42):21822–43.
[13] Wegener M, Isalgue A, Malmquist A, Martin A, Santarelli M, Arranz P, et al. Exergetic model of a small-scale, biomass-based CCHP/HP system for historic building structures. Energy Conversion and Management: X 2021;12:100148.
[14] Ghamari V, Hajabdollahi H, Dehaj MS. Comparison of gas turbine and diesel engine in optimal designof CCHP plant integrated with multi-effect and reverse osmosis desalinations. Process Saf Environ Prot 2021;154:505–18.
[15] Wei D, Ji J, Fang J, Yousefi N. Evaluation and optimization of PEM Fuel Cell-based CCHP system based on Modified Mayfly Optimization Algorithm. Energy Rep 2021;7:7663–74.
[16] Su B, Han W, Zhang X, Chen Y, Wang Z, Jin H. Assessment of a combined cooling, heating and power system by synthetic use of biogas and solar energy. Appl Energy 2018;229:922–35.
[17] Parikhani T, Azariyan H, Behrad R, Ghaebi H, Jannatkhah J. Thermodynamic and thermoeconomic analysis of a novel ammonia-water mixture combined cooling, heating, and power (CCHP) cycle. Renewable Energy 2020;145:1158–75.
[18] Peng M-P, Chen C, Peng X, Marefati M. Energy and exergy analysis of a new combined concentrating solar collector, solid oxide fuel cell, and steam turbine CCHP system. Sustainable Energy Technol Assess 2020;39:100713.
[19] Aghaei AT, Saray RK. Optimization of a combined cooling, heating, and power (CCHP) system with a gas turbine prime mover: A case study in the dairy industry. Energy 2021;229:120788.
[20] Ai T, Chen H, Jia J, Song Y, Zhong F, Yang S, et al. Thermodynamic analysis of a CCHP system integrated with a regenerative organic flash cycle. Appl Therm Eng 2022;202:117833.
[21] Afyon Biogas Electricity Generation Inc. (2016). Afyon-1 Biogas Electricity Production Plant Environmental Impact Assessment Report.
[22] Furubayashi T, Nakata T. Analysis of woody biomass utilization for heat, electricity, and CHP in a regional city of Japan. J Cleaner Prod 2021;290:125665.
[23] Imamović B, Halilčević SS, Georgilakis PS. Comprehensive fuzzy logic coefficient of performance of absorption cooling system. Expert Syst Appl 2022;190:116185.
[24] Köse Ö, Koç Y, Yağlı H. Performance improvement of the bottoming steam Rankine cycle (SRC) and organic Rankine cycle (ORC) systems for a triple combined system using gas turbine (GT) as topping cycle. Energy Convers Manage 2020;211:112745.
[25] Melikoglu M, Menekse ZK. Forecasting Turkey's cattle and sheep manure based biomethane potentials till 2026. Biomass Bioenergy 2020;132:105440.
[26] Stark M, Conti F, Saidi A, Zörner W, Greenough R. Steam storage systems for flexible biomass CHP plants-Evaluation and initial model based calculation. Biomass Bioenergy 2019;128:105321.
[27] Scaccabarozzi R, Tavano M, Invernizzi CM, Martelli E. Comparison of working fluids and cycle optimization for heat recovery ORCs from large internal combustion engines. Energy 2018;158:396–416.
[28] Bejan A, Tsatsaronis G, Moran MJ. Thermal design and optimization. John Wiley & Sons; 1995.
[29] Yang K, Zhu N, Ding Y, Chang C, Wang D, Yuan T. Exergy and exergoeconomic analyses of a combined cooling, heating, and power (CCHP) system based on dual-fuel of biomass and natural gas. J Cleaner Prod 2019;206:893–906.
[30] Aspen PlusV8.4. (2015). Engineering Economic Analysis Library.
[31] F-Chart Software. (2022). Genetic Method. https://www.fchart.com/ees/eeshelp/genetic_method.htm#:~:text=The%20genetic%20method%20implemented%20in,for%20Atmospheric%20Research%20(NCAR).&text=The%20genetic%20method%20intends%20to%20mimic%20the%20processes%20occurring%20in%20biological%20evolution. Access Date: 02.23.2022.
[32] Ghiasirad H, Asgari N, Khoshbakhti Saray R, Mirmasoumi S. Thermoeconomic assessment of a geothermal based combined cooling, heating, and power system, integrated with a humidification-dehumidification desalination unit and an absorption heat transformer. Energy Convers Manage 2021;235:113969.
[33] Parikhani T, Ghaebi H, Rostamzadeh H. A novel geothermal combined cooling and power cycle based on the absorption power cycle: Energy, exergy and exergoeconomic analysis. Energy 2018;153:265–77.
[34] Ghaebi H, Amidpour M, Karimkashi S, Rezayan O. Energy, exergy and thermoeconomic analysis of a combined cooling, heating and power (CCHP) system with gas turbine prime mover. Int J Energy Res 2011;35(8):697–709.